An estimation of the effect of a possible wind speed increase on the ocean mixed layer depth at the northern Patagonian continental shelf☆

Ezequiel Álvarez [a,b,*], Juan Zanella [a,b], Andrés Pescio [c], Walter Dragani [c,d]

[a] *International Center for Advanced Studies (ICAS), UNSAM, Campus Miguelete, 25 de Mayo y Francia, (1650) Buenos Aires, Argentina*
[b] *Departamento de Física, FCEyN, Universidad de Buenos Aires, Ciudad Universitaria, Pabellón I, (C1428EGA) Buenos Aires, Argentina*
[c] *Servicio de Hidrografía Naval, Ministerio de Defensa, Montes de Oca 2124, (C1270ABV) Buenos Aires, Argentina*
[d] *UMI IFAECI/CNRS - CONICET - UBA, Ciudad Universitaria, Pabellón II, 2do. Piso, (C1428EGA) Buenos Aires, Argentina*

ARTICLE INFO

ABSTRACT

A possible deepening of the ocean mixed layer is investigated at two selected points of the Patagonian continental shelf where a significant positive wind speed trend is estimated. Using a 1-dimensional vertical numerical model on a long term simulation (1979–2011) it is found that the mixed layer thickness presents a significant and positive trend of about 10 ± 1.5 cm/yr. The model is forced by atmospheric data from NCEP/NCAR 1 reanalysis and tidal constituents from TPXO 7.2 global model. Several numerical experiments are carried out in order to evaluate the impact of the different atmospheric variables considered in this study (wind components, air temperature, atmospheric pressure, specific humidity and cloud coverage). As a result it is found that a possible increase in the wind speed should be considered as a very significant factor for deepening the ocean mixed layer at the northern Patagonian continental shelf.

1. Introduction

Changes in wind due to global warming may have large geophysical impacts (McInnes et al., 2011). A number of changes in atmospheric processes have been reported at the Southwestern Atlantic Ocean. For instance, Barros et al. (2000) reported that the western border of the South Atlantic High and the atmospheric circulation over Southeastern South America have slowly shifted towards the south during the last decades. Changes in wind speed have a significant impact on storm surge and wind wave climates at the Southeastern South America continental shelf (see, for example, D'Onofrio et al., 2008; Dragani et al., 2010; Codignotto et al., 2012; Dragani et al., 2013). In addition, wind speed changes play a fundamental role in the spatial patterns of sea surface temperature warming, the global hydrological cycle (through evaporation) and in the regional distribution of sea level rise.

From Ekman (1905) to today many advances have been carried out for a better understanding of the dynamic of the mixed layer. Some of the main achievements in this subject were done during the 60 and 70's. For instance, Kraus and Turner (1967) were the first to heed the turbulent kinetic energy budget in a one-dimensional mixed layer model, using the approximately decoupled state of the equations for the thermal and mechanical energies. Later, Geisler and Kraus (1969) as well as Miropol'skiy (1970) and Denman (1973) included the viscous dissipation in the turbulent energy budget. Afterward Niiler (1975) showed that in addition to the equations for thermal (potential) and turbulent (kinetic) energy, an equation for the mean kinetic energy should be properly incorporated since entrainment converts some of the mean flow energy into turbulent energy, over and above the parameterized wind stress production. Important progress has been achieved in the theoretical understanding of the mixed layer during the last decades and, in particular, the development of 3-D ocean–atmosphere coupled model allowed to explore the vertical structure of the ocean in a more integral, complete and comprehensive way.

An increase in the wind speed has an important impact on the mean depth of the mixed layer of the shelf seas (Huang et al., 2006). The vertical structure of the water column is the result of ongoing competition between the buoyancy inputs due to surface heating and freshwater input, on the one hand, and stirring by the tides and wind stress, on the other. Variations in mixed layer depth affect the

---

rate of exchange between the atmosphere and deeper ocean, the capacity of the ocean to store heat and carbon and the variability of light and nutrients to support phytoplankton growth. However, the response of the Southern Ocean mixed layer to changes in the atmosphere is not well known (Sallée et al., 2010). On the Patagonian continental shelf the dominant buoyancy is mainly due to the seasonally varying surface heat (Guerrero and Piola, 1997) because the rainfall is very scarce. During the winter months, when heat is lost from the surface, the buoyancy term contributes to stirring by increasing surface density and making all or part of the water column convectively unstable. As a result the shelf waters are vertically well mixed during the winter months. This vertically mixed regime continues until the onset of positive heating at approximately the vernal equinox (September 21st in the southern hemisphere) after which the increasing input of positive buoyancy tends to stabilize the water column. Whether or not the water column stratifies depends on the relative strengths of the surface heating and the stirring due to frictional stresses imposed at the bottom boundary by the tidal flow and at the surface by wind stress. Huang et al. (2006) studied the decade variability of wind-energy input to the world ocean and found that this energy varied greatly on inter-annual to decal time scales. In particular, they showed that it has increased 12% over the past 30 years, and that the inter-annual variability mainly occurs in the latitude bands between 40°S and 60°S.

Direct observations collected over the Patagonian continental shelf waters (Argentina) indicate that during the 90's, winds were 20% stronger than during the 80's and that winds from the northwest direction were more frequent (Gregg and Conkright, 2002). In the region of study in this work (Fig. 1, left panel), a maximum wind speed trend greater than 2.5 cm s^{-1}/yr was estimated from NCEP/NCAR 1 reanalysis (NR1) at the border of the Patagonian continental shelf (at 44°S 60°W, approximately; Fig. 1, right panel).

The aim of this paper is to investigate and quantify a possible deepening of the mixed layer in a region of the Patagonian shelf where atmospheric and oceanographic data are available (Fig. 1, right panel) approximately at 44°S 61°W. We have studied two reference locations, A and B in Fig. 1, and found similar results for both of them. The study was carried out by means of a 1-dimensional numerical model (Sharples et al., 2006; Sharples, 1999) developed to study the physical structure of the upper layer of the ocean at coastal and shelf seas. This physical model employs a turbulence closure scheme to provide the link between local vertical stability (driven by seasonal solar heating) and the vertical turbulent mixing (driven by tidal currents and surface wind stress). This model was forced using atmospheric data from NR1 reanalysis and tidal constituents from TPXO 7.2 global model (see next section for details). Numerical results were conveniently validated using temperature profiles measured at four locations for three different dates, ranging from 1994 to 2006. The results obtained in this article are valid for the outer Northern Patagonian continental shelf, where the relevant atmospheric and oceanic conditions can be considered quite homogeneous, excluding tidal and shelf break fronts.

This region is ecologically and economically important. One of the most important economic activities in the area is fisheries, while its coastal marine fauna is practically unique in the world. The Patagonian shelf is characterized by a smooth slope and scarce relief features (Parker et al., 1997). The shelf broadens from north to south, ranging from 170 km at 38°S to more than 600 km south of 50°S. The main source of the shelf water masses is the sub-antarctic water flowing from the northern Drake Passage, through the Cape Horn Current (Hart, 1946) between the Atlantic coast and the Malvinas Islands, and the Malvinas Current in the eastern border of the shelf (Bianchi et al., 1982). The freshwater source

of the shelf is a small continental discharge. On the other hand, a low salinity water mass gets into the continental shelf through the Magellan Strait, where low salinity is due to high precipitation in the South Pacific, close to the west coast of Tierra del Fuego, and the melting of continental ice (Lusquiños, 1971; Lusquiños and Valdés, 1971; Piola and Rivas, 1997). South of 41°S, the shelf width is close to one quarter of the semi-diurnal tide wavelength, leading to favorable conditions for resonance (Piola and Rivas, 1997). The tidal amplitude in the Patagonian shelf is one of the highest in the world ocean (Kantha et al., 1995), and tidal currents are very energetic (Simionato et al., 2004).

2. Data

Surface (10 m height) zonal and latitudinal wind components, surface (2 m height) air temperature, surface atmospheric pressure, surface (2 m height) specific humidity, and cloud coverage from NR1 (period: 1979–2012) for node A (located at 44.7611°S 61.8750°W) and node B (42.8564°S 60°W) were used as atmospheric forcing of the model. The output from NR1 reanalysis is a set of grid data (Global T62 Gaussian grid) with a temporal resolution of 6 h. Data before 1979 were not included in this study due to known deficiencies of the reanalysis prior to satellite era, particularly in data-sparse regions such as the high-latitude Southern Hemisphere (Jones et al., 2009; Bromwich and Fogt, 2004). The main advantages of this reanalysis are its physical consistency and high temporal coverage. Full details of the NR1 project and the data set are given in Kalnay et al. (1996) and discussions on its quality in the Southern Hemisphere can be found in Simmonds and Keay (2000), among others. Since the behavior of nodes A and B are quite similar, in this paper we show the details of the calculations only for node A, whereas the final results are shown for both nodes.

The raw analysis of the NR1 data shows no temporal trend in variables, except in the wind (Pescio et al., 2015) where we find an increment of 1.7 ± 0.9 cm s^{-1}/yr at a 95% confidence level. The analogous result for the B node is 2.2 ± 0.9 cm s^{-1}/yr. In Fig. 2 is plotted the wind speed evolution at grid node A for the studied period of time.

To get a realistic representation of the tidal dynamics, tidal current constituents for five primary harmonic constituents (M2, S2, N2, O1, K1) at the grid node located at 44°S 61°W were obtained from TPXO 7.2 model (http://volkov.oce.orst.edu/tides/global.html). Tide computed from these five selected constituents account for almost all the real tide in the region. For instance, these constituents represent more than 98% of the total tidal energy when 51 harmonic constituents and the available sea level data series measured at Golfo Nuevo (Argentine Patagonia) are used. TPXO 7.2 is a recent version of a global model of ocean tides, which best-fits the Laplace Tidal Equations and along-track averaged data from TOPEX/Poseidon and Jason (on TOPEX/POSEIDON tracks since 2002) obtained with OTIS. The methods used to compute the model are described in detail by Egbert et al. (1994) and further by Egbert and Erofeeva (2002).

We used seven temperature quasi-continuous vertical profiles to validate the numerical simulations. Profiles gathered in 2006 were collected within the framework of the Coastal Contamination, Prevention and Marine Management project, which was part of the scientific agenda of the United Nations Development Program. Cruises were carried out on board the "Oca Balda" and "Puerto Deseado" oceanographic vessels, in March of 1994, 1996 and 2006. In each cruise, hydrographic stations were carried out along cross-shelf sections spanning the shelf from near-shore to the western boundary currents, between 38° and 55°S (Charo and Piola, 2014). For the purposes of this work, it has been used data collected at the following locations and dates (See Fig. 1):
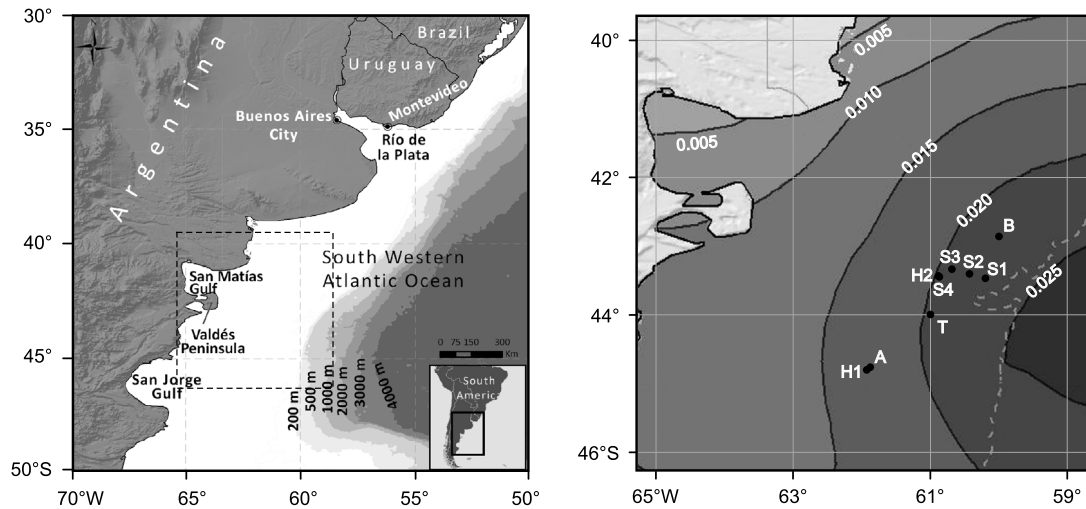
Fig. 1. *Left*: Region of study in this article. *Right*: Annual trend of sea surface wind speed in m s^{-1}/yr (contour solid lines); selected NR1 grid nodes for analysis (A and B); locations where water temperature profiles were measured (S1–S4); TPXO grid node (T); and HYCOM grid nodes (H1 and H2); 200 m contour is also indicated in gray dashed line. See text for details on each reference.
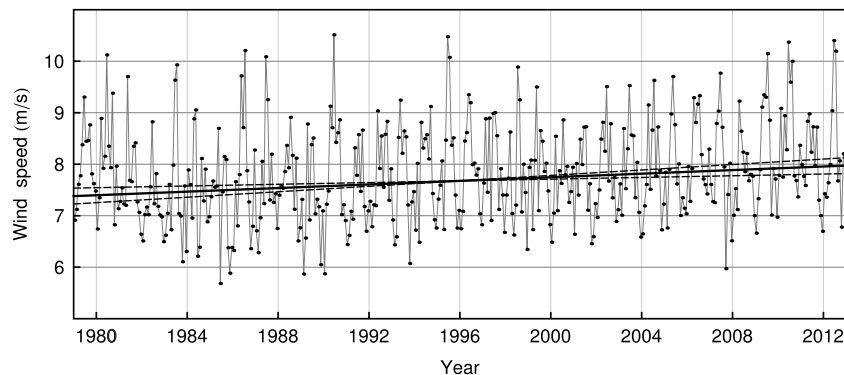

Fig. 2. Wind speed trend in the 1979–2012 studied period of time for node A. Each point represents the average wind speed of one month with data taken every 6 h. The Kendall–Theil algorithm yields a wind speed trend of 1.7 ± 0.9 cm s^{-1}/yr at a 95% confidence level. (The same result is obtained using a regular linear fit.) The solid line represents the average wind speed increase and the dashed lines its 95% confidence interval. The analogous result for the B node is 2.2 ± 0.9 cm s^{-1}/yr.

Name	Coordinates	Dates
S1	43.46°S 60.20°W	March 12th, 1994 & March 29th, 1996
S2	43.40°S 60.43°W	March 12th, 1994 & March 29th, 1996
S3	43.34°S 60.67°W	March 12th, 1994 & March 29th, 1996
S4	43.44°S 60.87°W	March 29th, 2006

Water depth at these locations varies between 97 and 104 m. In our simulations, the water depth was set to L = 97 m, corresponding to the site S4.

3. Numerical study of water column temperature profile and thermocline definition

In this section we describe the methods that yields the thermocline and mixed layer features using a 1-dimensional model.

Even though the 1-dimensional model does not take into account possible advection effects it is not a serious problem because previous works (Rivas and Piola, 2002; Rivas, 1990, 1994) have shown that not large advection effects should be expected in the selected region. On the other hand, the simulations show typically that at the end of the year the water temperature, though uniform, does not return to its exact initial value. The latter is

not a severe matter because our numerical experiments show that the maximum mixed layer depth is independent of the imposed initial sea surface temperature. We have tested the results of the 1-dimensional model against the HYbrid Coordinate Ocean (3-D) Model (HYCOM; see details in Halliwell et al., 2000; and Bleck, 2002) in the available period (2002–2012) of complete data of HYCOM global 1/12° reanalysis. We used data from two HYCOM grid nodes, $H1 = 44.80°S 61.92°W$, and $H2 = 43.44°S 60.88°W$; see Fig. 1.

We have found that the agreement between both models in the selected region and time lapse is very good within the required precision for this work. As a reference, in Fig. 3 there is a comparison of both models, and between our simulations and *in-situ* data for two selected dates as well. Similar results were obtained for the other available measured thermal profiles.

3.1. S2P3 numerical model

The program S2P3 is a 1-dimensional (vertical) coupled physical–biological numerical model. It uses meteorological data and tidal currents to simulate the 365-day evolution of several physical and biological variables within the water column. A detailed description can be found elsewhere (Sharples et al., 2006; Sharples, 1999).

By default, each run of the model starts on January 1st (day 1), when, for the northern hemisphere, the water column is

well mixed and has a uniform initial temperature. This initial water temperature must be provided by the user. As s2p3 model was developed to be used in the northern hemisphere some minor changes should be done to implement it in the southern hemisphere:

- The calendar must be shifted six months, which means that days must be numbered from 1 to 365 starting on July 1st. Our convention will be to name each of these 365-day periods according to the year in which they begin. For instance, 1995 must be understood as the period of 365 days beginning on July 1st, 1995 and ending on June 30th, 1996 (leap years will end on June 29th). This will be called the *the winter calendar.* Simulations span a period of 33 years, beginning on July 1st, 1979 and ending on June 29th, 2012.
- Since the calendar was shifted six months the sign of the latitude was inverted in order to reproduce the correct solar irradiance.
- To preserve the correct relative directions between the Coriolis force, wind stress, and tidal current, the latitudinal components of the tidal current and wind velocity should be inverted.

The water depth at the simulation site is 97 m. The numerical model divides the water column in n cells of equal thickness. Trade-off between resolution and computation time must be considered. After some preliminary tests, we carried out the bulk of our simulations using 100 cells, which resulted in smooth and consistent profiles.

The available meteorological data from NR1 had a resolution of 6 h, while the input for the numerical model takes only one daily value for each variable. For the surface air temperature, atmospheric pressure and specific humidity, the average of the four daily values from NR1 have been used. For cloud coverage, the average of the two daytime values have been used. Cloud coverage is also important during nighttime, because it affects heat losses. In any case, the difference between daytime and nighttime cloud coverage proved to be less than 5% on average. Concerning wind speed and direction, the four daily values provided by NR1 were used to compute a weighted average, such that the wind stress computed from this average is equal to the average of the stresses computed from the four daily values of the wind speed and direction. The initial winter water temperature was set equal to 6.8 °C, according to data collected by "Puerto Deseado" vessel on September 9th, 2006, at location S4 (Charo and Piola, 2014).

The model outputs vertical profiles for several variables, including water temperature and turbulent kinetic energy per unit mass. We used these two variables to define the thermocline boundaries and the mixed layer depth.

3.2. Model validation

We have made two independent validations of the model. In a first step we have compared the S2P3 1-dimensional model to the HYCOM 3-dimensional model for the 2002–2012 period. In order to quantify this comparison we have proceeded as follows. We have computed the temperature difference between both model profiles along the whole mixed layer during the stratification period (see below) for the ten years under study. We have normalized each computed difference by the temperature range in the profile in the corresponding day. The average of all these normalized relative temperature difference yields $16 \pm 7\%$, which we consider a good agreement between both models. In a second step, we have compared both models with available data of the temperature profile at S1–S4 locations (see Fig. 1). We show in Fig. 3 the outcome of the latter for reference locations S3 (March 12th, 1994) and S4 (March 29, 2006). We see that in both cases the agreement in surface and seabed is within 1°. The thermocline

limits are also well reproduced, except for S4 where a shift of approximately 10 m is found for the higher limit. Results obtained for S1 and S2 profiles are similar to those obtained for S3 and S4 profiles.

3.3. Study of temperature profiles: mixed layer and thermocline definition

We are interested at this point in defining the mixed layer for the water column, in order to study its properties and evolution at the studied locations from 1979 to 2011.

There are many algorithms which yield differently defined mixed layer and thermocline boundaries. These different definitions yield similar mixed layer or thermocline upper boundary for good contrast temperature profiles. The lower thermocline boundary, on the other hand, may yield some differences due to its relative smoothness in contrast to the upper boundary. In this work, the following three algorithms to define the mixed layer and thermocline boundaries have been used:

- *Temperature threshold*: We define the thermocline upper boundary as the depth at which the temperature decreases $0.1\Delta T$ with respect to the surface, where ΔT is the temperature difference between the surface and the seabed. Analogously, the lower boundary is defined as the depth at which the temperature increases by $0.1\Delta T$ with respect to the seabed. (See left panel in Fig. 4.)
- *Gradient scale*: The upper and lower boundaries are defined as the two depths at which the temperature gradient equals the mean temperature gradient between the surface and the seabed. (See central panel in Fig. 4.)
- *Turbulent kinetic energy (TKE)*: We define the thermocline as the region where TKE (per unit of mass) is less than or equal to a critical value. In fact, in the numerical model there is a minimum, fixed value for TKE, equal to 3×10^{-6} m^2 s^{-2}. The thermocline is the region where TKE takes this minimum value. With this definition, the mixed layer is the region next to the surface in which active turbulence is present. (See right panel in Fig. 4.)

In Fig. 4 the three different definitions for a typical summer day at noon can be seen. As it can be seen in the figure, the agreement for the mixed layer is very good, whereas the lower thermocline boundary may have some discrepancies which are not important because the aim of this work is to study the mixed layer depth and not the lower limit of the thermocline. We will proceed using simultaneously all three thermocline definitions and verify that our conclusions are independent of which one is used. We also note that there is relatively little hour-to-hour variation within a given day. In the rest of this paper the mixed layer depth for each day is defined as the average of the 24 depth values computed from the hourly outputs of the numerical model.

To study the annual stability of the mixed layer depth definitions, the direct outcome of the three definitions is plotted and compared for each day of the year 2008 of the winter calendar (Fig. 5, top panel). Similar results were obtained for all the simulated years. In the bottom panel of the figure, the period between days 138 and 302 has been selected to do a moving average of 15 days for the mixed layer depth. In this period the thermocline has been formed and all three methods have a better agreement since there is a good contrast in the temperature profile.

In the following sections we study the mixed layer depth and its time evolution along the years for a selected time window of the winter calendar.
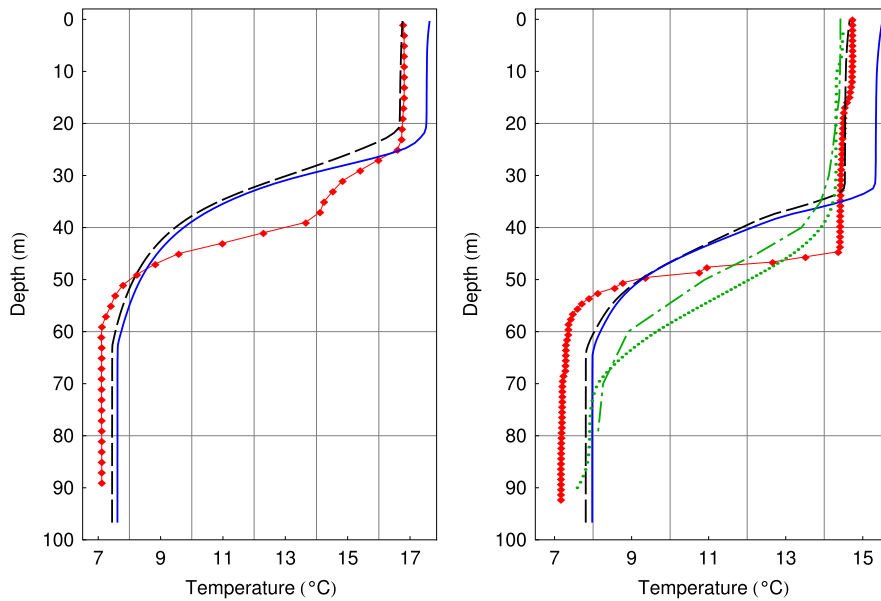
Fig. 3. Reference plots for the validation of the 1-dimensional S2P3 numerical model. All cited locations are shown in Fig. 1. *Left*: March 12th, 1994 temperature profiles obtained from the 1-dimensional S2P3 model for locations A (black dashed) and B (blue solid line), compared with *in situ* data for location S3 (red diamonds). *Right*: March 29, 2006 temperature profiles obtained from the 1-dimensional S2P3 model. Analogous references as in the left panel, but the location corresponds to S4, and in this case is also shown the temperature profiles retrieved from the HYCOM 3-dimensional model for locations H1 (green dash-dotted) and H2 (green dotted). (For interpretation of the references to color in this figure legend, the reader is referred to the web version of this article.)
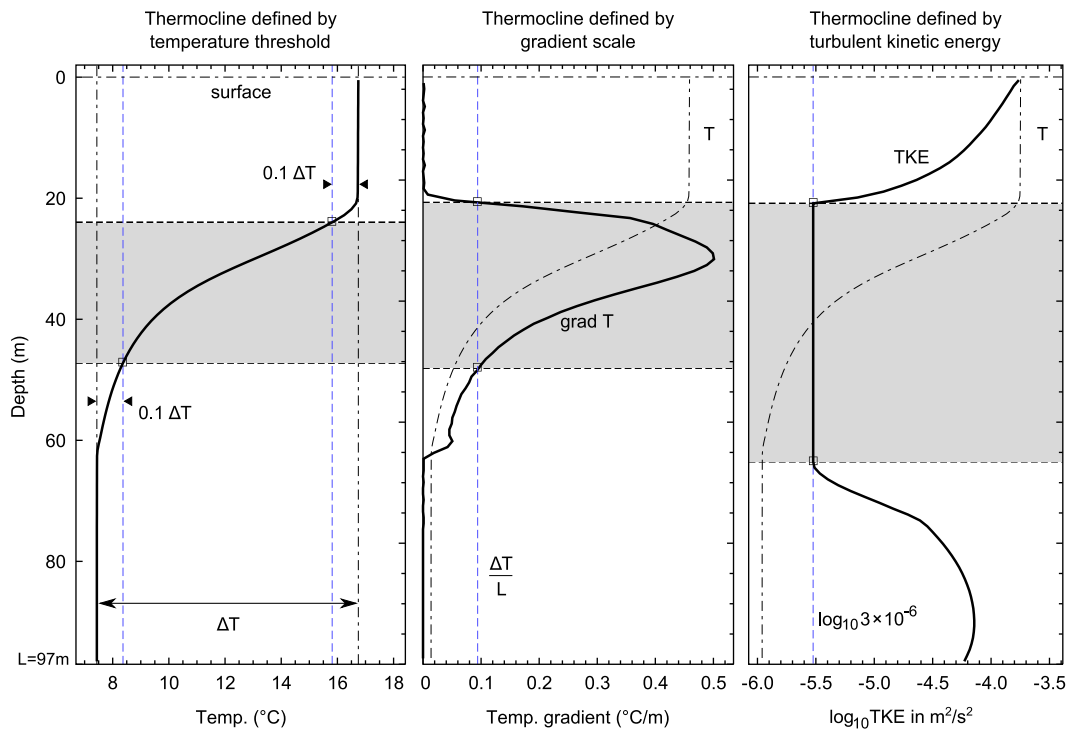

Fig. 4. Outcome of the three thermocline definitions (see text) for the same summer day at noon. The white upper region corresponds to the mixed layer, the shaded region to the thermocline, and the bottom region to the deep water region. All three definitions, although quite different, yield a similar mixed layer region. ΔT is the temperature difference between surface and seabed, and $L = 97$ m is the depth of the seabed.

4. Analysis of mixed layer depth and its trend

Using the previous mixed layer definitions, as well as the time period in the year in which its depth is relatively robust to meteorological fluctuations, we study in this section the mixed layer depth evolution in the 1979–2011 33-year period. We show the results in this section using the TKE mixed layer definition, although any definition would work as well. In any case, we

stress that similar results are obtained when the other two mixed layer definitions are used. We analyze the mixed layer depth evolution for six reference days within the 138–302 days period. To diminish the impact of weather fluctuations, for each of these reference days we average the mixed layer depth in an interval going from the previous 7 days to the following 7 days. This yields for each reference day a set of 33 points – one for each year – with an average mixed layer depth. Since each year has a
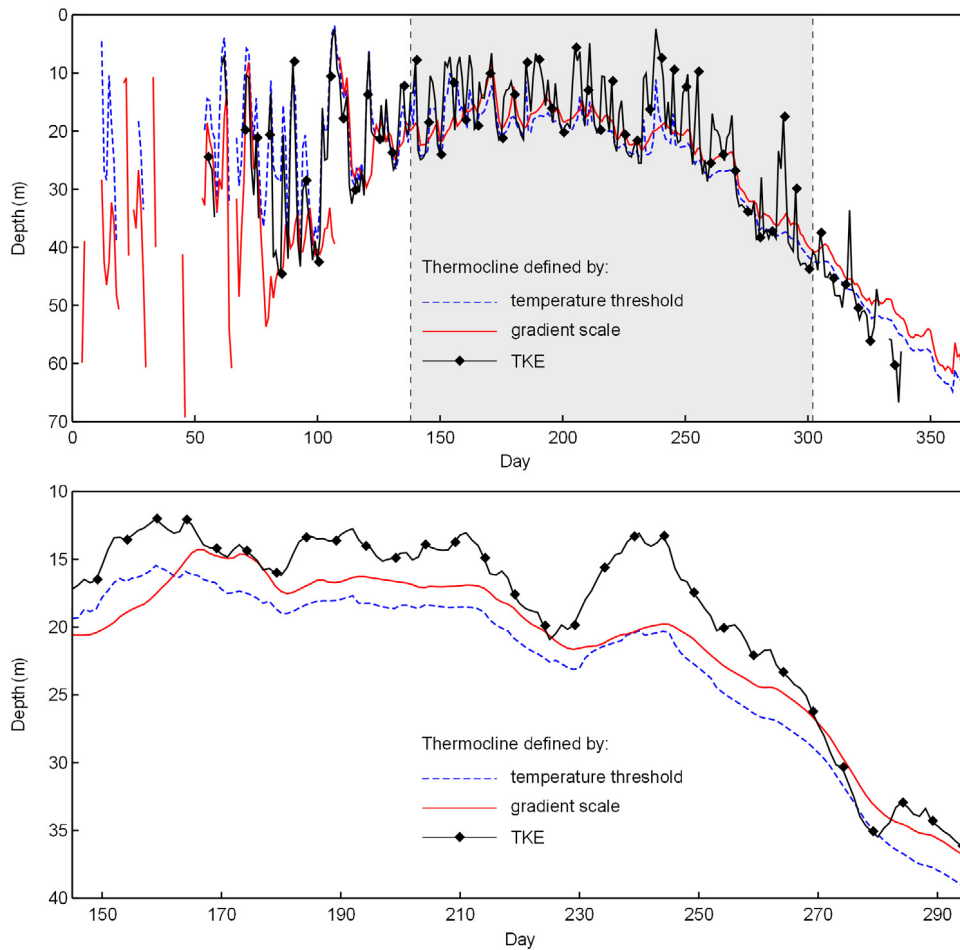
Fig. 5. *Top*: Mixed layer depth for a given complete year using the three thermocline definitions. *Bottom*: selected time window between days 138 and 302, when the contrast reached in water temperature yields an outcome more stable to weather fluctuations. In the bottom plot a 15-day moving average has been applied to soften the curves.

fluctuating different weather, we do not expect to see a pattern in this set of 33 points. However, if these fluctuations lie on a smoothly changing function, we can expect that a linear fit in each of these sets eliminates the fluctuations and gives us a hint on the first derivative of this smoothly changing function for each of the reference days.

In Fig. 6 we show the results of this analysis and we found that for all six reference days the linear fit yields a positive (in depth) slope with a significance that ranges from approximately one to three standard deviations of the fit.

Motivated by this first set of results, which shows a clear positive trend in the mixed layer depth, we proceed to find the average trend of this depth for the full time window in which the mixed layer depth is relatively stable to weather fluctuations. In this sense, we take 11 bins of 15 days each, from day 138 to day 302, and compute the slope of the mixed layer depth as described in the previous paragraph. To have the full average variation, we do an average on these 11 slopes, and obtain a final result of 10.1 ± 1.4 cm/yr and 10.0 ± 1.7 cm/yr for reference locations A and B, as it can be seen in Fig. 7. This result, being one of the most important in the article, would indicate a clear trend of increasing mixed layer depth along the years by more than ~7 standard deviations. It is worth noticing at this point that the other two mixed layer definitions yield similar results: 11.1 ± 1.2 cm/yr (temperature threshold) and 10.6 ± 1.1 cm/yr (gradient scale).

On the other hand, the HYCOM model has been running for only 10 years, which is not enough to compute reliable trends in mixed layer depth. In fact, the HYCOM trend for the mixed layer depth yields 50 ± 21 cm/yr which, although compatible at a 1.8σ level, it could be misleading to compare it to the output of 33 years of the 1D model. We point out that the 10-year trend using the 1D model yields 10 ± 10 cm/yr, which yields a compatibility level of 1.7σ.

5. Discussion

Different numerical experiments were carried out in order to analyze the sensitivity of our results. In a first experiment, we have used the 1979 wind data for all the 1979–2011 period, leaving the rest of the meteorological variables in its original values. On the other hand, in a second experiment, we have used the original wind data for each year, but the rest of meteorological variables have been left with the 1979 data for all the years in the 1979–2011 period. We then performed the same analysis that yielded Fig. 7, but for these two experiments, and reached the results shown in Fig. 8 for location A. We have found that in the first scenario there is no significant trend of the mixed layer depth (1.4 ± 0.5 cm/yr), whereas in the second scenario we retrieve a very similar result to the one with the actual meteorological conditions (9.9 ± 1.3 cm/yr). These results would be isolating the change in the wind as the main cause of the increase trend in the mixed layer depth. To strength this conclusion, in Fig. 9 we have plotted the mean wind speed versus the mixed layer mean depth during the stratification season for site A. This plot confirms not only a correlation between these two variables, but also a trend of recent years to have deeper mixed layer and stronger winds.(Similar results were obtained for location B). Notice that even though the
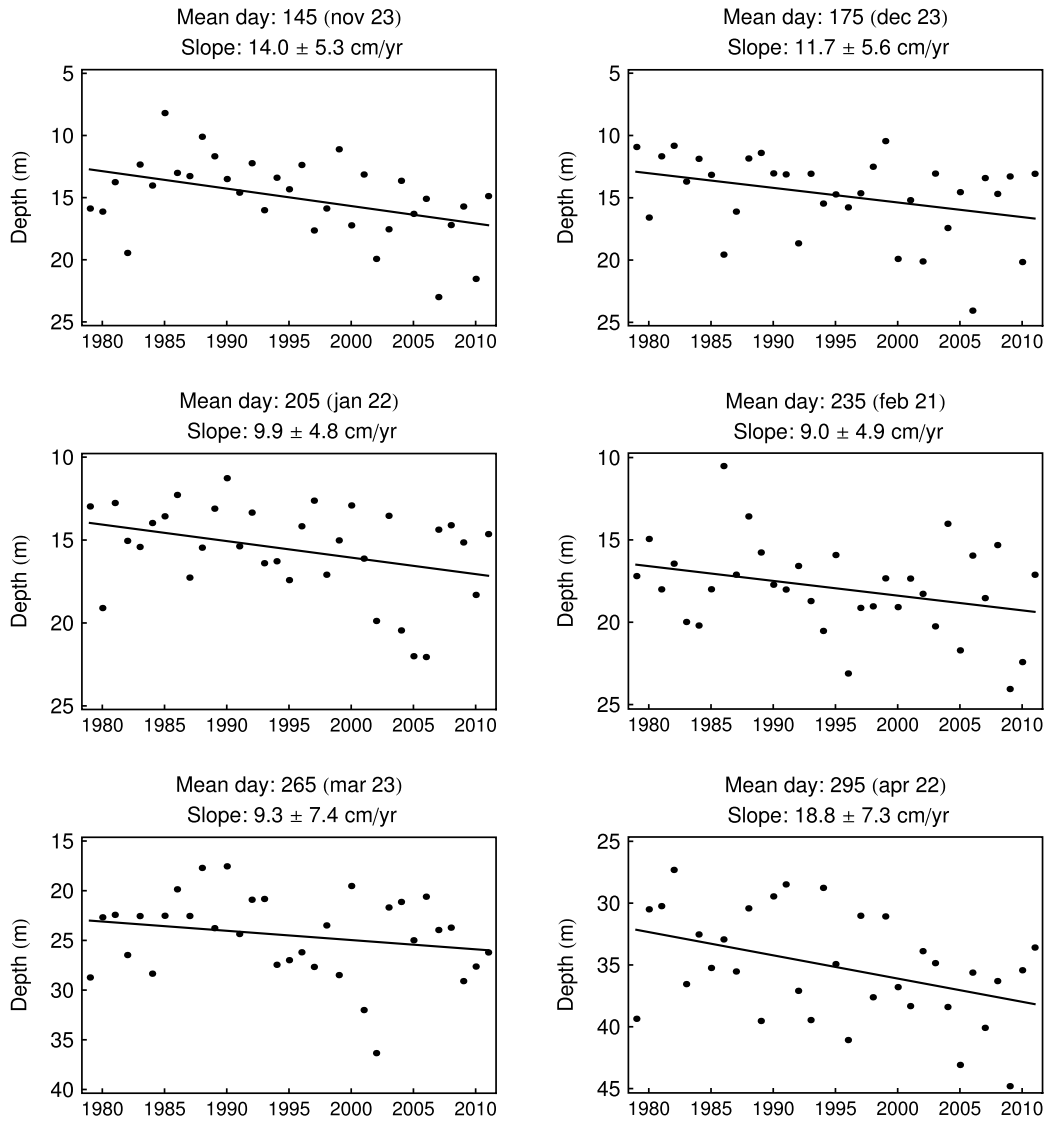
Fig. 6. Fit to the mixed layer depth at location A as a function of the years for six reference days within the time window determined in Fig. 5. Each point represents the average of the mixed layer depth in the 15 days surrounding the given day.
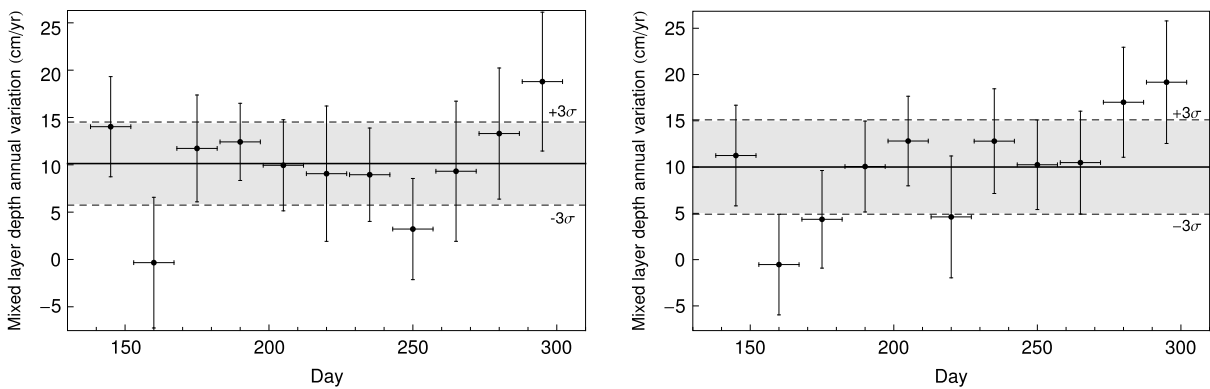

Fig. 7. Fit to the mixed layer depth annual variation for 11 equally long bins in the 138–302 days time window during the 1979–2011 period. The outcome of the fit is 10.1 ± 1.4 cm/yr and 10.0 ± 1.7 cm/yr for reference locations A (left panel) and B (right panel), respectively, which is more than 7 standard deviations different from zero.

mixed layer depth depends on the wind stress, and this last on a non-linear function of the wind speed, the relationship between the annual mean wind speed and the mixed layer mean depth has a good linear fit (Fig. 9) because wind speeds have a small spread between 6.5 and 7.9 m/s.

Finally, it is important to remark that because the present data set is only 33 years long, it is not possible to distinguish between a steadily increasing or simply the upward portion of a multidecadal oscillation. Only a longer data set will be able to separate these possibilities.
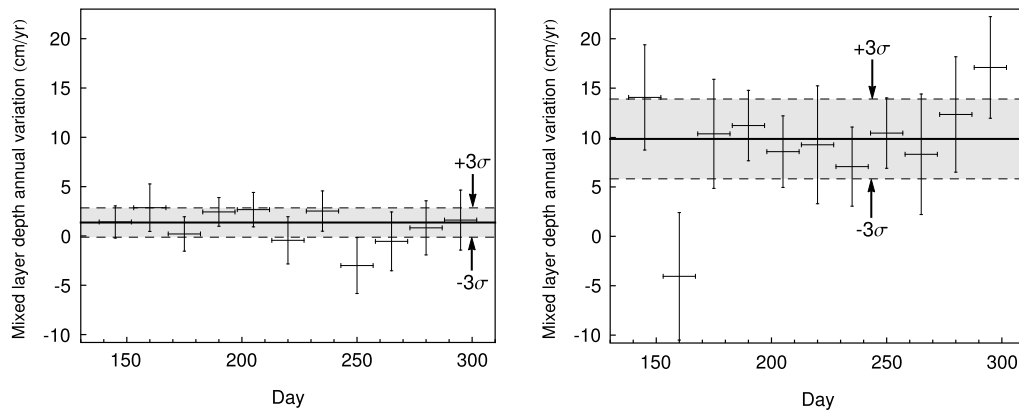
Fig. 8. Same analysis as in Fig. 7 for reference location A, but for two experiments. *Left*: in all years the wind has been set to its 1979 value leaving all other variables in its real values. *Right*: the wind in each year has been left in its real value, but all other variables have been set to their 1979 values for all years. These plots suggest that the wind would be the major cause of the increase trend found in Fig. 7.
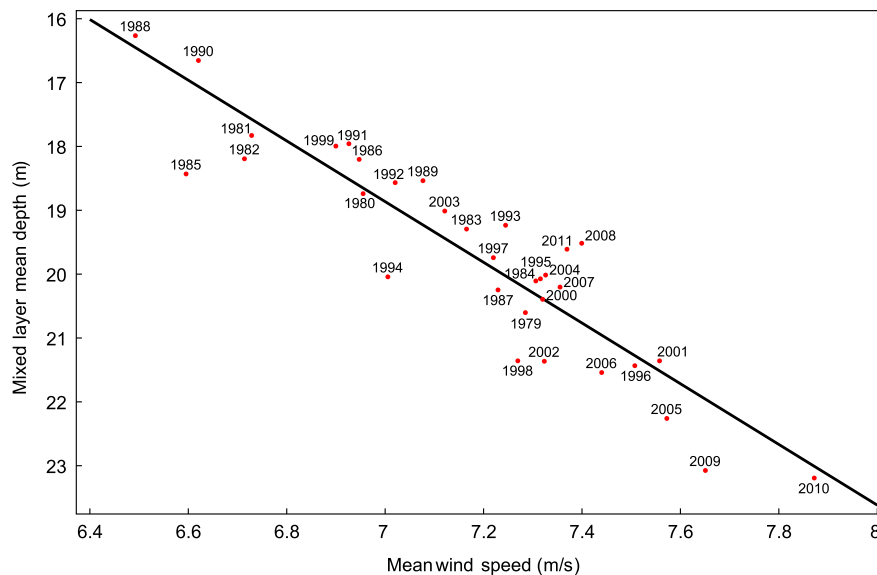

Fig. 9. Scattered plot for the mean wind speed versus the mixed layer mean depth during the stratification season for each of the studied years for location A. The correlation between these two variables can be seen by a linear fit on them which yields the solid line in the plot with a slope equal to 4.8 ± 0.4 cm/(cm s^{-1}). Pearson correlation coefficient is 0.916. Notice the accumulation of recent years in the bottom right of the figure.

6. Conclusions

A possible deepening of the ocean mixed layer at the northern Patagonian continental shelf (Fig. 1, left panel) has been investigated and quantified by means of a 1-dimensional (vertical) numerical model (Sharples et al., 2006; Sharples, 1999) forced by atmospheric data from NCEP/NCAR 1 (NR1) and tidal current constituents from TPXO 7.2 global model. The performance of the model was analyzed by means of two comparisons: in a first step the outcome of the model was compared to the HYbrid Coordinate Ocean (3-D) Model (HYCOM) in the period of time in which the latter was available, 2002–2012; and in a second step the results of the simulation were compared to observed temperature profiles at four locations for three different dates, ranging from 1994 to 2006. In both cases it was concluded that the model is reliable for simulating the vertical thermal structure in the region (Fig. 3). Numerical simulations and experiments were carried out at two locations of the Patagonian continental shelf, corresponding to two grid points of the NR1 reanalysis (points A and B on the right panel of Fig. 1). These points belong to a region where a significant positive wind speed trend has been previously detected (Fig. 1, right panel, and Fig. 2). Three different criteria were tested to

determine objectively the thickness and evolution of the simulated mixed layer, showing compatibility between them (Figs. 4 and 5).

From a long term numerical simulation (1979–2011) it was found that the mixed layer thickness showed a significant and positive trend which seems to be noticeably variable along the year (Fig. 6). In addition, the mean mixed layer depth trend computed from the 33 simulated years, which could be considered as a representative value of the mixed layer thickness trend for the region, resulted equal to 10 ± 1 cm/yr and 10 ± 2 cm/yr (Fig. 7) for the two studied locations, respectively. It should be noted the lowest trend in mixed layer depth is appreciated around day 160 in Fig. 7, which correspond to the first week of December. It is interesting to notice that December also presents the lowest positive monthly wind speed trend (0.7 cm s^{-1}/yr) which could explain the lowest mixed layer trend value observed around day 160. In order to analyze the sensitivity of these results additional numerical experiments were carried out. A numerical experiment was carried out using real atmospheric input for the 1979–2011 period, with exception of the wind speed which was set to values corresponding to 1979. As a result, no significant trend was obtained (Fig. 8 left panel). On the contrary, another numerical experiment was carried out using real wind speed for

the 1979–2011 period, but setting the additional atmospheric input to values corresponding to 1979. In this second case, a significant positive trend – similar to real data – was obtained (Fig. 8 right panel). This clearly supports the hypothesis that the wind speed is the most likely factor deepening the ocean mixed layer at the northern Patagonian continental shelf. This is also shown in Fig. 9, where a correlation between a deeper mixed layer and a stronger wind can be appreciated.

Acknowledgments

References

Barros, V., Castañeda, M.E., Doyle, M., 2000. Recent precipitation trends in Southern South America to the East of the Andes: an indication of a mode of climatic variability. In: Smolka, P., Volkheimer, W. (Eds.), Southern Hemisphere Paleo and Neoclimates Concepts, Methods, Problems. Springer, Berlin, pp. 187–206.

Bianchi, A.A., Massonneau, M., Olivera, R.M., 1982. Análisis estadístico de las características T-S del sector austral de la plataforma continental argentina. Acta Oceanogr. Argent. 3 (1), 93–118.

Bleck, R., 2002. An oceanic general circulation model framed in hybrid isopycnic-Cartesian coordinates. Ocean Model. 37, 55–88.

Bromwich, D.H., Fogt, R.L., 2004. Strong trends in the skill of the ERA-40 and NCEP-NCAR reanalyses in the high and middle latitudes of the Southern Hemisphere, 1958–2001. J. Clim. 17, 4603–4619.

Charo, M., Piola, A.R., 2014. Hydrographic data from the GEF patagonia cruises. Earth Syst. Sci. Data 6, 265–271. http://dx.doi.org/10.5194/essd-6-265-2014.

Codignotto, J., Dragani, W.C., Martin, P.B., Simionato, C.G., Medina, R.A., Alonso, G., 2012. Wind-wave climate change and increasing erosion observed in the outer Rí o de la Plata, Argentina. Cont. Shelf Res. 38, 110–116. http://dx.doi.org/10.1016/j.csr.2012.03.013.

Denman, K.L., 1973. A time-dependent model of the upper ocean. J. Phys. Oceanogr. 3, 173–184.

D'Onofrio, E., Fiore, M., Pousa, J.L., 2008. Changes in the regime of storm surges at Buenos Aires, Argentina. J. Coast. Res. 24, 260–265. http://dx.doi.org/10.2112/05-0588.1.

Dragani, W.C., Martin, P.B., Alonso, G., Codignotto, J., Prario, B., Bacino, G., 2013. Wind wave climate change: Impacts on the littoral processes at the northern Buenos Aires coast, Argentina. Clim. Change 121, 649–660. http://dx.doi.org/10.1007/s10584-013-0928-8.

Dragani, W.C., Martin, P.B., Campos, M.I., Simionato, C., 2010. Are wind wave heights increasing in South-eastern South American continental shelf between 32°S and 40°S? Cont. Shelf Res. 30, 481–490. http://dx.doi.org/10.1016/j.csr.2010.01.002.

Egbert, G., Bennett, A., Foreman, M., 1994. TOPEX/POSEIDON tides estimated using a global inverse model. J. Geophys. Res. 99, 24821–24852. http://dx.doi.org/10.1029/94JC01894.

Egbert, G., Erofeeva, S.Y., 2002. Efficient inverse modeling of barotropic ocean tides. J. Atmos. Ocean. Technol. 19, 183–204. http://dx.doi.org/10.1175/1520-0426(2002)019<0183:EIMOBO>2.0.CO2.

Ekman, V.W., 1905. On the influence of the earths rotation on ocean currents. Ark. Mat. Astron. Fys. 2 (11), 1–53.

Geisler, J.E., Kraus, E.B., 1969. The well-mixed Ekman boundary layer. Deep-Sea Res. 16 (Suppl.), 73–84.

Gregg, W.W., Conkright, M.E., 2002. Decadal changes in global ocean chlorophyll. Geophys. Res. Lett. 29, 1730–1734. http://dx.doi.org/10.1029/2002GL014689.

Guerrero, R.A., Piola, A.R., 1997. Masas de agua en la plataforma continental. In: Boschi E.E. (ed) El Mar Argentino y sus Recursos Pesqueros, Antecedentes Históricos de las Exploraciones en el Mar y las Caracterí sticas Ambientales, vol. 1, Inst. Nac. Invest. Desarrollo Pesquero, Mar del Plata, Argentina, pp. 107–118.

Halliwell, G.R., Bleck, R., Chassignet, E.P., Smith, L.T., 2000. Mixed layer model validation in Atlantic Ocean simulations using the hybrid coordinate ocean model, HYCOM. Evol. Smooth 80, OS304.

Hart, T.J., 1946. Report on trawling survey of the Patagonian continental shelf. Discov. Rep. 23, 223–408.

Huang, R.X., Wang, W., Liu, L.L., 2006. Decadal variability of wind-energy input to the world ocean. Deep Sea Res. Part II 53, 31–41. http://dx.doi.org/10.1016/j.dsr2.2005.11.001.

Jones, J.M., Fogt, R.L., Gareth, M.W., Marshall, J., Jones, P.D., Visbeck, M., 2009. Historical SAM variability. Part I: Century-length seasonal reconstructions. J. Clim. 22, 5319–5345. http://dx.doi.org/10.1175/2009JCLI2785.1.

Kalnay, E., Kanamitsu, M., Kistler, R., Collins, W., Deaven, D., Gandin, L., Iredell, M., Saha, S., White, G., Woollen, J., Zhu, Y., Leetmaa, A., Reynolds, B., Chelliah, M., Ebisuzaki, W., Higgins, W., Janowiak, J., Mo, K., Ropelewski, C., Wang, J., Jenne, R., Joseph, D., 1996. The NCEP/NCAR 40-Year reanalysis project. Bull. Am. Meteorol. Soc. 77, 437–471. http://dx.doi.org/10.1175/1520-0477(1996)077<0437:TNYRP>2.0.CO2.

Kantha, L.H., Tierney, C., Lopez, J.W., Desai, S.D., Parke, M.E., Drexler, L., 1995. Barotropic tides in the global ocean from a nonlinear tidal model assimilating altimetric tides: 2. Altimetric and geophysical implications. J. Geophys. Res. 100, 25309–25317. http://dx.doi.org/10.1029/95JC02577.

Kraus, E.B., Turner, J.S., 1967. A one-dimensional model of the seasonal thermocline, part II. Tellus 19, 98–105.

Lusquiños, A.J., 1971. Algunas características de las aguas de la plataforma continental argentina, in Datos y Resultados de las Campañas Pesquería, Pesquería X, Ser. Inf. Tec., Publ. 10/X, edited by S. F. Villanueva, Proyecto de Desarrollo Pesquero, Mar del Plata, Argentina.

Lusquiños, A.J., Valdés, A.J., 1971. Aportes al conocimiento de las masas de agua del Atlántico Sudoccidental, Rep. H659. Serv. de Hidrografía Nav., Buenos Aires, Argentina, p. 48.

McInnes, K.L., Erwin, T.A., Bathols, J.M., 2011. Global Climate Model projected changes in 10 m wind speed and direction due to anthropogenic climate change. Atmos. Sci. Lett. 12, 325–333. http://dx.doi.org/10.1002/asl.341.

Miropol'skiy, Y.A., 1970. Nonstationary model of the wind-convection mixing layer in the ocean. Izv. Atmos. Ocean. Phys. 6 (12), 1284–1294.

Niiler, P.P., 1975. Deepening of the wind-mixed layer. J. Marine Res. 33 (3), 405–422.

Parker, G., Paterlini, M.C., Violante, R., 1997. El fondo marino. In: Boschi EE (ed) El Mar Argentino y sus Recursos Pesqueros, Antecedentes Históricos de las Exploraciones en el Mar y las Caracterí sticas Ambientales, vol. 1. Inst. Nac. Invest. Desarrollo Pesquero, Mar del Plata, Argentina, pp. 65–87.

Pescio, A.E., Martín, P., Dragani, W., 2015. Wind speed trends over the Southeastern continental shelf of South America, between 33° and 50°S. Int. J. Climatol. 36 (1), 501–507. http://dx.doi.org/10.1002/joc.4348.

Piola, A.R., Rivas, A.L., 1997. Corrientes en la Plataforma Continental. In: Boschi, E.E. (ed) El Mar Argentino y sus Recursos Pesqueros, Antecedentes Históricos de las Exploraciones en el Mar y las Caracterí sticas Ambientales, vol. 1, Inst. Nac. Invest. Desarrollo Pesquero, Mar del Plata, Argentina, pp. 119–132.

Rivas, A.L., 1990. Heat balance and annual variation of mean temperature in the North Patagonian gulfs. Oceanol. Acta 13, 265–272.

Rivas, A.L., 1994. Spatial variation of the annual cycle of temperature in the Patagonian shelf between 40 and 50° of south latitude. Cont. Shelf Res. 14, 1539–1554. http://dx.doi.org/10.1016/0278-4343(94)90089-2.

Rivas, A.L., Piola, A.R., 2002. Vertical stratification of shelf off northern Patagonia. Cont. Shelf Res. 22, 1549–1558. http://dx.doi.org/10.1016/S0278-4343(02)00011-0.

Sallée, J.B., Speer, K.G., Rintoul, S.R., 2010. Zonally asymmetric response of the Southern Ocean mixed-layer depth to the Southern Annular Mode. Nat. Geosci. 3, 273–279. http://dx.doi.org/10.1038/ngeo812.

Sharples, J., 1999. Investigating the seasonal vertical structure of phytoplankton in shelf seas. Mar. Model. 1, 3–38. http://dx.doi.org/10.1016/S0079-6611(99)00002-6.

Sharples, J., Ross, O.N., Scott, B.E., Greenstreet, S.P.R., Fraser, H., 2006. Inter-annual variability in the timing of stratification and the spring bloom in the North-western North Sea. Cont. Shelf Res. 26, 733–751. http://dx.doi.org/10.1016/j.csr.2006.01.011.

Simionato, C., Dragani, W.C., Nuñez, M.N., Engel, M., 2004. A set of 3-D nested models for tidal propagation from the Argentinean Continental Shelf to Río de la Plata Estuary-Part I. M$_2$. J. Coast. Res. 20, 893–912. http://dx.doi.org/10.2112/1551-5036(2004)20[893:ASODNM]2.0.CO2.

Simmonds, I., Keay, K., 2000. Mean Southern Hemisphere extratropical cyclone behavior in the 40-year NCEP-NCAR reanalysis. J. Clim. 13, 873–885. http://dx.doi.org/10.1175/1520-0442(2000)013<0873:MSHECB>2.0.CO2.